

MATHEMATICAL ANALYSIS OF BLOOD FLOW THROUGH AN ARTERIAL SEGMENT WITH TIME-DEPENDENT STENOSIS

J.C. MISRA, S.D. ADHIKARY and G.C. SHIT

Department of Mathematics, Indian Institute of Technology
Kharagpur-721302, India
E-mail: jcm@maths.iitkgp.ernet.in

Received December 11, 2007; revised March 5, 2008; published online September 9, 2008

Abstract. A mathematical model is developed here with an aim to study the pulsatile flow of blood through an arterial segment having a time-dependent stenosis. Blood is considered to consist of a core layer where erythrocytes are concentrated and a peripheral plasma layer that is free from erythrocytes. The plasma layer is taken to behave as a Newtonian fluid, while the core layer is represented by a Casson fluid (non-Newtonian) model. The pulsatile flow is analyzed by considering a periodic pressure gradient, which is a function of time. A perturbation analysis is employed to solve the governing differential equations by taking the Womersley frequency parameter to be small ($\alpha < 1$). This is a realistic assumption for physiological fluid flows, particularly for flow of blood in small vessels. Using appropriate boundary conditions, analytical expressions for the velocity profile, the volumetric flow rate, the wall shear stress and the flow resistance have been derived. These expressions are computed numerically and the computational results are presented graphically, in order to illustrate the variation of different quantities that are of particular interest in the study.

Key words: Pulsatile flow, Casson model, Two-layer model, Time-dependent stenosis.

1 INTRODUCTION

The laminar flow of blood in arteries with time-dependent stenosis plays an important role in the diagnosis and clinical treatment as well as in the fundamental understanding of many cardiovascular diseases. To understand the effects of stenosis in the lumen of an artery, many researchers [5, 7, 10, 13, 22, 23] investigated the flow of blood through stenosed arteries by treating blood as a Newtonian fluid. However, experimental studies show that in the vicinity of a stenosis, the shear rate of blood is low and therefore the non-Newtonian behavior of blood is quite prominent. The non-Newtonian flow behavior of blood

for steady flow in stenosed arteries was studied by Misra et al.[14] as well as by Chaturani and Samy [4], by treating blood as a Herschel-Bulkley fluid model. Shukla et al.[17] dealt with the effects of stenosis on non-Newtonian flow of blood in an artery by considering power-law model.

Let us introduce the following notations: r^* is the radial co-ordinate, z^* is the axial co-ordinate, $R^*(z, t)$ denotes the radius of the artery, $R_0^*(z, t)$ is the radius of core region, $R_p^*(z, t)$ denotes the radius of plug region, L^* is the length of the artery, L_0^* is the length of the stenosis, d^* denotes the distance of the onset of stenosis from the vertical axis, a is the characteristic radius, ρ is the density of blood, μ denotes the viscosity of blood, τ^* is the shear stress of blood, τ_y is the yield stress, p^* denotes the blood pressure, α denotes the Womersley parameter, A is the amplitude of the flow, w is the angular frequency.

It is known that blood flow in the human circulatory system is caused by the pumping action of the heart, which in turn produces a pressure gradient throughout the system. Tu and Deville [21] presented a theoretical analysis of pulsatile flow of blood in stenosed arteries, where the non-Newtonian behavior of blood was taken to be of Herschel-Bulkley type. Cassonova and Giddens [1] as well as Young and Tsai [24] experimentally investigated the pulsatility of blood flow through arterial stenosis, while several other researchers [3, 15, 19] theoretically carried out the pulsatile flow of a single-layer non-Newtonian fluid past on arterial stenosis. Sud and Sekhon [20] presented a mathematical model of flow in a single artery subject to a pulsating pressure gradient as well as body acceleration. A mathematical analysis was carried out by Misra and Ghosh [11] with an aim to study the velocity field for the pulsatile flow of blood in a porous elastic vessel of variable cross-section.

Two-layer models of steady flow of blood through stenosed arteries were studied by Halder *et al.* [8] and Shukla *et al.* [18]. Sharan and Popel [16] investigated a two-phase model for blood flow in narrow tubes. Gupta *et al.* [6] developed a three layered semi-empirical model for blood flow and particulate suspension through narrow tubes, while Misra and Ghosh [12] formulated and analyzed a three layered model of blood flow in branched arteries.

The aim of the present investigation has been to study the effect of a time-dependent stenosis on pulsatile flow of blood considered as a two-layered fluid. The peripheral plasma layer is considered as a Newtonian fluid, while the core layer that contains erythrocytes is represented by a Casson fluid depicting the non-Newtonian behavior of blood, in conformity to the experimental observation of Charm and Kurland [2]. A perturbation technique has been developed for solving the problem analytically. The derived analytical expressions are computed in order to examine the variation of the velocity profile, the volumetric flow rate, the radius of the core region, the wall shear stress and the resistance to the blood flow.

2 Formulation of the Problem

Let us consider an axially symmetric, laminar, pulsatile and fully developed flow of blood through a circular artery having a stenosis (see Fig.1). Cylindrical polar coordinates (r^*, ϕ^*, z^*) , with the pole located on the axis of artery have

been used to analyze the problem.

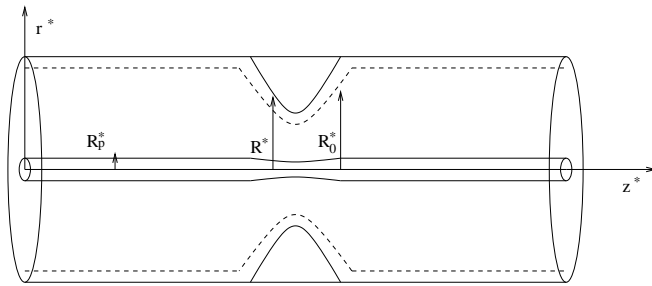


Figure 1. Schematic diagram of multiphase blood flow in a stenosed artery.

The momentum equation is given by

$$\rho \frac{\partial u^*}{\partial t^*} = -\frac{\partial p^*}{\partial z^*} - \frac{1}{r^*} \frac{\partial(r^* \tau^*)}{\partial r^*}. \tag{2.1}$$

The Casson constitutive equation describing the non-Newtonian behavior of blood may be written as

$$\tau^{*\frac{1}{2}} = \left[-\mu \frac{\partial u^*}{\partial r^*} \right]^{\frac{1}{2}} + \tau_y^{\frac{1}{2}}, \quad \tau^* > \tau_y, \tag{2.2}$$

$$-\frac{\partial u^*}{\partial r^*} = 0, \quad \tau^* \leq \tau_y. \tag{2.3}$$

The theoretical analysis takes care of the two-phase flow of blood, the peripheral plasma layer is considered to be Newtonian, while the core region that is supposed to contain all the erythrocytes contained in the blood inside the artery is treated as non-Newtonian. The mathematical model that is developed here is formulated by the following set of equations:

$$\tau^* = -\mu \frac{\partial u^*}{\partial r^*}, \quad \text{if } R_0^*(z^*, t^*) < r^* < R^*(z^*, t^*), \tag{2.4}$$

$$\tau^{*\frac{1}{2}} = \left[-\mu \frac{\partial u^*}{\partial r^*} \right]^{\frac{1}{2}} + \tau_y^{\frac{1}{2}}, \quad \text{if } R_p^*(z^*, t^*) < r^* < R_0^*(z^*, t^*), \tag{2.5}$$

$$-\frac{\partial u^*}{\partial r^*} = 0, \quad \text{if } 0 < r^* < R_p^*(z^*, t^*), \tag{2.6}$$

along with the boundary conditions

$$u^* = 0 \quad \text{at } r^* = R^*(z^*, t^*), \tag{2.7}$$

$$\tau^* \text{ is finite at } r^* = 0. \tag{2.8}$$

These equations are to be supplemented by the condition of continuity of u^* and τ^* at the interfaces $r^* = R_0^*(z^*, t^*)$ and $r^* = R_p^*(z^*, t^*)$.

The pressure gradient which is a function of z^* and t^* , is represented as

$$\frac{\partial}{\partial z^*} p^*(z^*, t^*) = -q^*(z^*) f(t^*)$$

with $q^*(z^*) = -\frac{\partial}{\partial z^*} p^*(z^*, 0)$, $f(t^*) = 1 + A \sin(\omega t^*)$.

For the analysis presented in the sequel, we use the following non-dimensional variables

$$\begin{aligned} z &= \frac{z^*}{a}, \quad r = \frac{r^*}{a}, \quad R(z, t) = \frac{R^*(z^*, t^*)}{a}, \quad R_0(z, t) = \frac{R_0^*(z^*, t^*)}{a}, \\ R_p(z, t) &= \frac{R_p^*(z^*, t^*)}{a}, \quad \tau = \frac{2\tau^*}{q_0 a}, \quad \theta = \frac{2\tau_y}{q_0 a}, \quad u = \frac{u^*}{q_0 a^2 / 4\mu}, \quad t = t^* \omega, \\ Q(z, t) &= \frac{Q^*(z, t)}{\pi q_0 a^4 / 8\mu}, \quad d = \frac{d^*}{a}, \quad \delta = \frac{\delta^*}{a}, \quad L_0 = \frac{L_0^*}{a}, \quad L = \frac{L^*}{a}, \\ \alpha^2 &= \frac{a^2 \omega}{\mu / \rho}, \quad q(z) = \frac{q^*(z^*)}{q_0}. \end{aligned} \quad (2.9)$$

where q_0 is a constant pressure gradient (which is negative).

In terms of these non-dimensional variables, equation (2.1) reads

$$\alpha^2 \frac{\partial u}{\partial t} = 4q(z)f(t) - 2\frac{1}{r} \frac{\partial(r\tau)}{\partial r}, \quad 0 < r < R(z, t), \quad (2.10)$$

while the equations (2.4)–(2.8) take the forms

$$-\frac{\partial u}{\partial r} = 2\tau, \quad R_0(z, t) < r < R(z, t), \quad (2.11)$$

$$-\frac{\partial u}{\partial r} = 2\left[\theta + \tau - 2\sqrt{\tau\theta}\right], \quad R_p(z, t) < r < R_0(z, t), \quad (2.12)$$

$$-\frac{\partial u}{\partial r} = 0, \quad 0 < r < R_p(z, t), \quad (2.13)$$

$$u = 0 \quad \text{at} \quad r = R, \quad \tau \text{ is finite at } r = 0. \quad (2.14)$$

Also u and τ have to be continuous at $r = R_0(z, t)$ and $r = R_p(z, t)$. The geometry of the stenosis in non-dimensional form is given by

$$R(z, t) = \begin{cases} 1 - A_1(t) \left[L_0^{(m-1)}(z-d) - (z-d)^m \right], & \text{if } d \leq z \leq d + L_0, \\ 1, & \text{otherwise} \end{cases}$$

with

$$A_1(t) = \frac{\delta \left[1 - e^{(-t/T)} \right] m^{\frac{m}{m-1}}}{a L_0^m (m-1)}, \quad m \neq 1$$

here δ denotes the maximum height of the stenosis, the maximum height being attained at $z = d + L_0/m^{1/m-1}$. The volumetric flow rate is given by

$$Q(z, t) = 4 \int_0^{R(z, t)} r u(z, r, t) dr.$$

3 Analytical Solution of the Problem

Considering the Womersley parameter to be small, the velocity u , shear stress τ as well as R_0 and R_p can be expressed in the following form

$$u(z, r, t) = u_0(z, r, t) + \alpha^2 u_1(z, r, t) + \dots \tag{3.1}$$

$$\tau(z, r, t) = \tau_0(z, r, t) + \alpha^2 \tau_1(z, r, t) + \dots \tag{3.2}$$

$$R_0(z, r, t) = R_{00}(z, r, t) + \alpha^2 R_{10}(z, r, t) + \dots \tag{3.3}$$

$$R_p(z, r, t) = R_{0p}(z, r, t) + \alpha^2 R_{1p}(z, r, t) + \dots \tag{3.4}$$

Using (3.1) and (3.2) in (2.10), we have

$$\frac{\partial}{\partial r}(r\tau_0) = 2rq(z)f(t), \tag{3.5}$$

$$\frac{\partial u_0}{\partial t} = -\frac{2}{r} \frac{\partial}{\partial r}(r\tau_1). \tag{3.6}$$

Integrating (3.5) and using the boundary condition (2.14), we have

$$\tau_0 = q(z)f(t)R_p, \quad 0 \leq r \leq R_p. \tag{3.7}$$

In the regions $R_p \leq r \leq R_0$ and $R_0 \leq r \leq R$, the continuity of τ_0 at R_{0p} and R_{00} yields

$$\tau_0 = q(z)f(t)r. \tag{3.8}$$

Introducing (3.1) and (3.2) into equations (2.11)–(2.13) and equating like powers of α we obtain

$$-\frac{\partial u_0}{\partial r} = 2\tau_0, \quad -\frac{\partial u_1}{\partial r} = 2\tau_1, \quad \text{if } R_0 \leq r \leq R, \tag{3.9}$$

$$\begin{aligned} -\frac{\partial u_0}{\partial r} &= 2\left[\theta + \tau_0 - 2\sqrt{\theta\tau_0}\right], \\ -\frac{\partial u_1}{\partial r} &= 2\tau_1\left[1 - \sqrt{\frac{\theta}{\tau_0}}\right], \end{aligned} \quad \text{if } R_p \leq r \leq R_0, \tag{3.10}$$

$$\frac{\partial u_0}{\partial r} = 0, \quad \frac{\partial u_1}{\partial r} = 0, \quad \text{if } 0 \leq r \leq R_p. \tag{3.11}$$

The boundary conditions for u_0 and u_1 are:

$$u_0 = 0, \quad u_1 = 0 \quad \text{at } r = R, \tag{3.12}$$

$$u_0, \quad u_1 \text{ are continuous at } R_{00} \text{ and } R_{0p}.$$

From (3.8), (3.9) and (3.12) we have

$$u_0 = q(z)f(t)(R^2 - r^2), \quad R_0 \leq r \leq R. \tag{3.13}$$

Using (3.12) in (3.8) and (3.10), one can find

$$\begin{aligned} u_0 &= 2\theta(R_{00} - r) + q(z)f(t)(R_{00}^2 - r^2) - \frac{8}{3}\sqrt{\theta q(z)f(t)}(R_{00}^{3/2} - r^{3/2}) \\ &\quad + q(z)f(t)(R^2 - R_{00}^2), \quad R_p \leq r \leq R_0. \end{aligned} \tag{3.14}$$

Now from (3.8), (3.11), (3.12) and (3.14) we have

$$u_0 = 2\theta(R_{00} - R_{0p}) + q(z)f(t)(R_{00}^2 - R_{0p}^2) - \frac{8}{3}\sqrt{\theta q(z)f(t)}(R_{00}^{3/2} - R_{0p}^{3/2}) + q(z)f(t)(R^2 - R_{00}^2), \quad 0 \leq r \leq R_p. \quad (3.15)$$

Neglecting the squares and higher powers of α in (3.4) and using (3.7), one obtains

$$r|_{\tau_0=\theta} = R_{0p} := \frac{\theta}{q(z)f(t)}. \quad (3.16)$$

Again, making use of the regularity condition that τ_1 is finite at $r = 0$, equation (3.15) along with (3.6) gives

$$\tau_1 = - \left[\theta(R_{00} - R_{0p}) + \frac{q(z)f'(t)}{2}(R_{00}^2 - R_{0p}^2) - \frac{4}{3}\sqrt{\frac{\theta q(z)}{f(t)}}f'(t)(R_{00}^{3/2} - R_{0p}^{3/2}) \right] R_{0p} - \frac{q(z)f'(t)R_{0p}}{4}(R^2 - R_{00}^2), \quad 0 \leq r \leq R_p.$$

The continuity of τ_1 at $r = R_{0p}$ yields

$$\tau_1 = - \left[\theta \left(R_{00} \frac{r}{2} - \frac{r^2}{3} \right) + \frac{q(z)f'(t)}{2} \left(R_{00}^2 \frac{r}{2} - \frac{r^3}{4} \right) - \frac{4}{3}\sqrt{\frac{\theta q(z)}{f(t)}}f'(t) \left(R_{00}^{3/2} \frac{r}{2} - \frac{2r^{5/2}}{7} \right) \right] - \frac{q(z)f(t)}{2}(R^2 - R_{00}^2)\frac{r}{2} + \frac{A_2}{r}, \quad R_p \leq r \leq R_0,$$

the expression for A_2 is given in the Appendix.

Similarly, since τ_1 is continuous at R_0 , we have

$$\tau_1 = - \frac{q(z)f'(t)}{2} \left(R^2 \frac{r}{2} - \frac{r^3}{4} \right) + \frac{A_3}{r}, \quad R_0 \leq r \leq R,$$

where A_3 stands for a quantity whose expression is presented in the Appendix. Using (3.12), the equations (3.9)–(3.11) give rise to

$$u_1 = - \frac{q(z)f'(t)}{2} \left(\frac{R^4}{4}(r^2 - R^2) - \frac{1}{16}(r^4 - R^4) \right) + A_3 \log \left(\frac{r}{R} \right), \quad R_0 \leq r \leq R, \\ u_1 = X(r), \quad R_p \leq r \leq R_0, \\ u_1 = X(R_{0p}), \quad 0 \leq r \leq R_p. \quad (3.17)$$

The expressions for velocity in the peripheral and core layers can now be calculated by using the equations (3.1), (3.13)–(3.15) and (3.17).

We note that the yield plane, which was initially located at $r = R_{0p}$ will be displaced by a distance $\alpha^2 R_{1p}$. The new location of the yield plane can be described mathematically by the equation

$$\tau^2(R_{0p} + \alpha^2 R_{1p}) = \theta^2.$$

Expanding it in Taylor's series about R_{0p} and using $\tau_0(R_{0p}) = \theta$, we have

$$R_{1p} = -\frac{\tau_1(R_{0p})}{p(z)f(t)} = -\frac{1}{p(z)f(t)} \left[\left\{ \theta(R_{00} - R_{0p}) + \frac{q(z)f'(t)}{2}(R_{00}^2 - R_{0p}^2) - \frac{4}{3} \sqrt{\frac{\theta q(z)}{f(t)}} f'(t)(R_{00}^{3/2} - R_{0p}^{3/2}) \right\} R_{0p} - \frac{q(z)f'(t)}{2}(R^2 - R_{00}^2) \right]. \quad (3.18)$$

Using (3.4), (3.16) and (3.18) we have the expression for R_p as

$$R_p = \frac{1}{q(z)f(t)}\theta - \alpha^2 \frac{1}{q(z)f(t)} \left(\left\{ \theta(R_{00} - R_{0p}) + \frac{q(z)f'(t)}{2}(R_{00}^2 - R_{0p}^2) - \frac{4}{3} \sqrt{\frac{\theta q(z)}{f(t)}} f'(t)(R_{00}^{3/2} - R_{0p}^{3/2}) \right\} R_{0p} - \frac{q(z)f'(t)}{2}(R^2 - R_{00}^2) \right). \quad (3.19)$$

The volumetric flow rate can be computed from (18) by re-writing it in the form

$$Q(z, t) = 4 \left(u(z, R_p, t) \frac{R_p^2}{2} + \int_{R_p}^{R_0} ru(z, r, t) dr + \int_{R_0}^R ru(z, r, t) dr \right). \quad (3.20)$$

Different expressions for $u(z, r, t)$ can to be used for the different regions.

The value of the wall shear stress τ_w is a quantity that is of particular importance from the physiological point of view. It is given by

$$\tau_w = (\tau_0 + \alpha^2 \tau_1)|_{r=R} = q(z)f(t)R + \alpha^2 \left(-\frac{q(z)f'(t)R^3}{16} + \frac{A_3}{R} \right).$$

The value of R_{00} in (3.3) is found by using the continuity of u_0 at R_{00} . In doing so, we have used the Newton-Raphson method, by taking the non-dimensional velocity in the peripheral layer at R_{00} as its value in the steady case, i.e. 0.03. In order to determine the value of R_{10} , we consider the equation

$$\tau^2(R_{00} + \alpha^2 R_{10}) = \tau_0^2(R_{00}). \quad (3.21)$$

The value of R_{10} can be obtained by expanding the left side of (3.21) in Taylor's series about R_{00} . The resistance to the flow can be calculated by using the formula

$$\lambda = (P_0 - P_L)/Q(z, t), \quad (3.22)$$

where pressure $p = P_0$ at $z = 0$ and $p = P_L$ at $z = L$.

It may be noted that if we write $u = u_0 + \alpha^2 u_1$ and use (3.13)–(3.15) and (3.17), we find that the right hand side of (3.20) involves the unknown quantity $q(z)$. The quantities $Q(z, t)$ and $q(z)$ in (3.20) are both unknown. In order to determine $q(z)$ one may choose the value of $Q(z, t)$ as its value in the steady state. By considering $\theta/q(z)f(t) \ll 1$ and using (3.20), we find

$$q(z) = \frac{Q_s}{R^4} + \frac{16}{7} \left(\frac{\theta Q_s}{R^5} \right)^{\frac{1}{2}} + \frac{64\theta}{49R}, \quad \text{where } R = R(z, t). \quad (3.23)$$

While computing $q(z)$, one may take $Q_s = 1.0$ (cf. Shukla et al.[17]). After $q(z)$ is determined, $Q(z, t)$ can be calculated from (3.20).

Integrating (3.23) with respect to z between the limits 0 to L and multiplying by $f(t)$ we find the value of $(P_0 - P_L)$ and then calculate the resistance of blood flow, λ by using (3.22).

4 Results and Discussion

The motivation behind developing this mathematical model has been to study some aspects of multiphase flow of blood through an artery having a time-dependent stenosis. For the purpose of numerical computation of the quantities of interest, we have performed a thorough quantitative analysis, by taking the following values of the different parameters involved in the present study:

$$a = 0.5mm, \quad L = 30, \quad L_0 = 10, \quad d = 10, \quad \theta = 0.05, \quad A = 0.7, \\ \delta = 0.1, \quad \alpha^2 = 0.049, \quad m = 2.0, \quad T = 1.0.$$

In order to understand the complete nature of the time dependent stenosis, the computed numerical results are plotted in Figs.2 and 3.

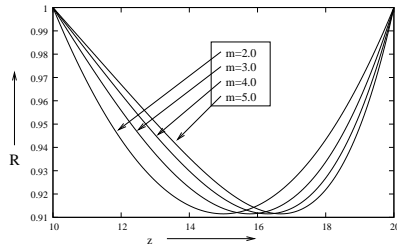


Figure 2. Change of the shape of stenosis for different values of m at $t/T = 1.0$.

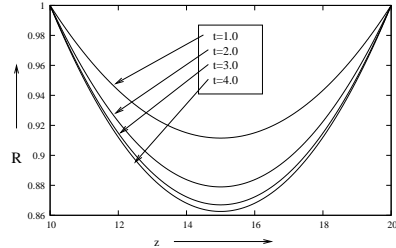


Figure 3. Change in the shape of the stenosis as time progresses (when $m = 2$ and $T = 1.0$).

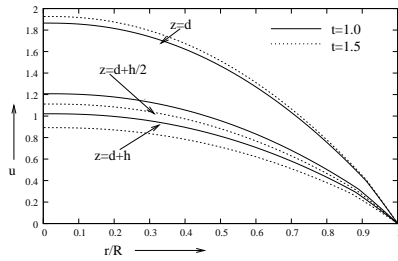


Figure 4. Radial distribution of blood velocity at different axial distances (where $h = L_0/m^{1/m-1}$, $m = 2.0$, $A = 0.2$).

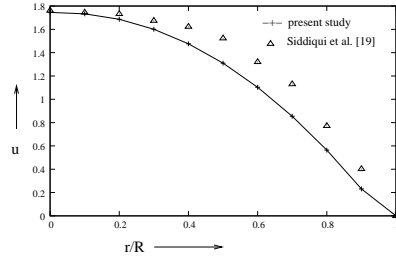


Figure 5. Comparison of velocities with Siddiqui et al. [19] in the non-stenosis region for $A = 0.2$, $\theta = 0.01$, $t = 0.78$.

Fig. 2 shows the shape of the stenosis for different values of the parameter $m \geq 2$ for a particular time period $t/T = 1.0$. It may be observed that the geometry of the stenosis is symmetric for $m = 2.0$ and that the symmetry is

disturbed as the value of m increases. In Fig. 3 we have illustrated the change in the shape of the stenosis with the advancement of time.

Variation of the velocity of blood in the radial direction at different axial positions and at different instants of time is shown in Fig. 4. This figure reveals that the velocity decreases as r increases and further that the velocity decreases as the axial distance z increases from the onset of the stenosis up to the peak of the stenosis.

Fig.5 gives a comparison of our results with those reported by Siddiqui et al.[19]. The reason for the differences in the results is two-fold. In our study we have considered multi-phase flow of blood and the stenosis to be time-dependent, while in [19], blood flow was treated as a single phase flow and the stenosis was assumed to be independent of time.

Fig. 6 gives the variation of the volumetric flow rate with time for different values of the amplitude (A) at a given yield stress (θ). This figure shows that at all instants of time, the volumetric flow rate increases with the increase in amplitude. Fig. 7 gives the time-variation of the volumetric flow rate for different values of the yield stress for a given amplitude.

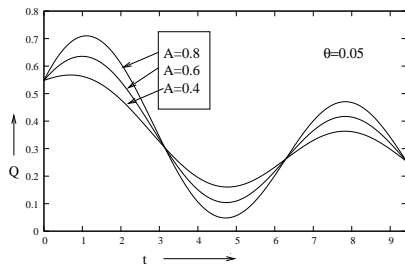


Figure 6. Variation of volumetric flow rate with time for different values of A at $z = d + h/2$, $h = L_0/m^{1/m-1}$.

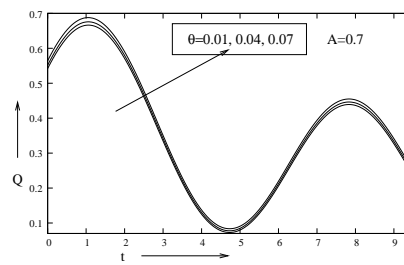


Figure 7. Variation of volumetric flow rate with time for different values of θ at $z = d + h/2$, $h = L_0/m^{1/m-1}$.

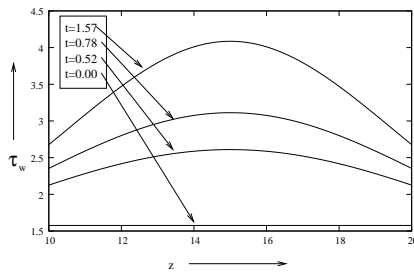


Figure 8. Variation of wall shear stress with z for different values of time at $A = 0.7$, $\theta = 0.05$.

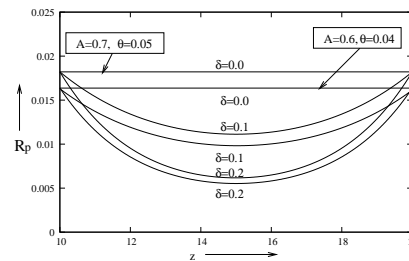


Figure 9. Variation of radius of plug core layer with z for different values of A , θ and δ .

Fig. 8 reveals that in the stenosed portion of the artery, the wall shear stress increases with the increase in axial distance and also that at a given distance, it increases with the passage of time. Karino and Goldsmith [9] made an observation that the wall shear stress helps to determine the sites where the

platelets aggregate.

The variation of the radius in the plug region of the stenosed portion is illustrated in Fig. 9 for particular values of the amplitude and the yield stress. This figure shows that at a particular axial distance, as the value of δ (the height of the stenosis at $t = 0$) increases, the radius of the plug flow zone decreases.

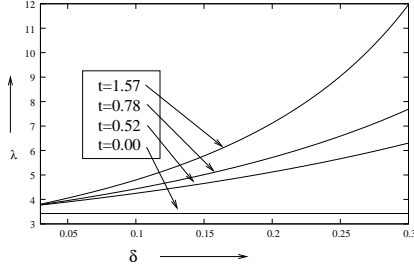


Figure 10. Variation of resistance of the flow with δ for different values of time at $z = d + h/2$, $h = L_0/m^{1/m-1}$, $A = 0.7$, $\theta = 0.05$.

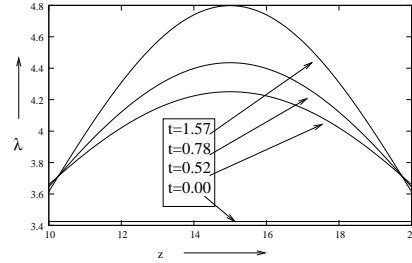


Figure 11. Variation of resistance of the flow with z for different values of time at $\theta = 0.05$, $A = 0.7$.

Fig. 10 shows that the resistance to flow increases with the increase in δ and that for a particular value of δ , the flow resistance increases as time progresses. From Fig. 11 one may further conclude that at any instant of time, the flow resistance attains its maximum at the throat of the stenosis. This figure also reveals that the flow resistance in the stenosed portion of the artery increases with time.

Acknowledgment

The authors are thankful to the CSIR, New Delhi for their financial support.

Appendix

$$A_2 = - \left[\frac{\theta R_{0p}}{2} \left(R_{00} - \frac{4}{3} R_{0p} \right) + \frac{q(z)f'(t)R_{0p}}{4} \left(R_{00}^2 - \frac{3}{2} R_{0p}^2 \right) \right. \\ \left. - \frac{4}{3} \sqrt{\frac{\theta q(z)}{f(t)}} \frac{f'(t)R_{0p}}{2} \left(R_{00}^{3/2} - \frac{10}{7} R_{0p}^{3/2} \right) \right] - \frac{q(z)f'(t)}{2} (R^2 - R_{00}^2) \frac{R_{0p}}{2},$$

$$A_3 = - \left[\frac{\theta R_{00}}{6} - \frac{q(z)f'(t)R_{00}^3}{16} - \frac{6}{21} \sqrt{\frac{\theta q(z)}{f(t)}} f'(t) R_{00}^{5/2} \right] R_{00} + A_2,$$

$$X(r) = 2 \left[\theta \left(\frac{R_{00}}{4} (r^2 - R_{00}) - \frac{1}{9} (r^2 - R_{00}^2) \right) + \frac{q(z)f'(t)}{2} \left(\frac{R_{00}}{2} (r^2 - R_{00}^2) \right) \right. \\ \left. - \frac{1}{16} (r^4 - R_{00}^4) - \frac{4}{3} \sqrt{\frac{\theta q(z)}{f(t)}} f'(t) \left(\frac{R_{00} 63/2}{2} (r^2 - R_{00}^2) - \frac{4}{49} (r^{7/2} - R_{00}^{7/2}) \right) \right]$$

$$\begin{aligned}
 & + \frac{q(z)f'(t)}{4}(R^2 - R_{00}^2)(r^2 - R_{00}^2) - 2A_2 \log\left(\frac{r}{R_{00}}\right) \\
 & + 2\sqrt{\frac{\theta}{q(z)f(t)}} \left[\theta \left(\frac{R_{00}}{3}(r^{3/2} - R_{00}^{3/2}) - \frac{2}{15}(r^{5/2} - R_{00}^{5/2}) \right) \right. \\
 & - \frac{q(z)f'(t)}{2} \left(\frac{R_{00}^2}{3}(r^{3/2} - R_{00}^{3/2}) - \frac{1}{14}(r^{7/2} - R_{00}^{7/2}) \right) \\
 & - \frac{4}{3} \sqrt{\frac{\theta q(z)}{f(t)}} f'(t) \left(\frac{R_{00}^{3/2}}{3}(r^{3/2} - R_{00}^{3/2}) - \frac{2}{21}(r^3 - R_{00}^3) \right) \\
 & \left. + \frac{q(z)f'(t)}{12}(R^2 - R_{00}^2)(r^{3/2} - R_{00}^{3/2}) - 2A_2 \left(\frac{1}{r^{1/2}} - \frac{1}{R_{00}^{1/2}} \right) \right] \\
 & + \frac{q(z)f'(t)}{4} \left(\frac{R^4}{4}(R_{00}^2 - R^2) - \frac{1}{16}(R_{00}^4 - R^4) \right) + A_3 \log\left(\frac{R_{00}}{R}\right).
 \end{aligned}$$

References

- [1] R.A. Cassanova and D.P. Giddens. Disorder distal to modeled stenosed in steady and pulsatile flow. *J. Biomech.*, **11**:441–453, 1978.
- [2] S. Charm and G. Kurland. Viscometry of human blood for shear rates 0-10,000 sec^{-1} . *Nature*, **206**:617–618, 1965.
- [3] P. Chaturani and R. Pannalagar. Pulsatile flow of Casson's fluid through stenosed arteries with application to blood flow. *Biorheology*, **23**:499–511, 1986.
- [4] P. Chaturani and R.P. Samy. A study of non-Newtonian aspects of blood flow through stenosed arteries and its applications in arterial diseases. *Biorheology*, **22**:521–531, 1985.
- [5] J.H. Forrester and D.F. Young. Flow through a converging and diverging tube and the implication in occlusive vascular disease. *J. Biomech.*, **3**:127–316, 1970.
- [6] B.B. Gupta, K.M. Nigam and M.Y. Jaffrin. A three-layer semi-empirical model for flow of blood and other particulate suspensions through narrow tubes. *J. of Biomech. Eng.*, **104**:129–135, 1982.
- [7] K. Halder. Oscillatory flow of blood in stenosed artery. *Bull. math. Biology*, **49**(3):279–287, 1987.
- [8] K. Halder and H.I. Andersson. Two-layered model of blood flow through stenosed arteries. *Acta Mech.*, **117**:221–228, 1996.
- [9] T. Karino and H.L. Goldsmith. Flow behavior of blood cells and rigid spheres in annular vortex. *Philos.Trans.R.Soc.London*, **B279**:413–445, 1977.
- [10] D.A. McDonald. On steady flow through modeled vascular stenosis. *J. Biomech*, **12**:13–20, 1979.
- [11] J.C. Misra and S.K. Ghosh. Flow of a Casson fluid in a narrow tube with a side branch. *Int. J. Eng. sci.*, **38**:2045–2077, 2000.
- [12] J.C. Misra and S.K. Ghosh. Pulsatile flow of a viscous fluid through a porous elastic vessel of variable cross-section: A mathematical model for hemodynamic flows. *Comput. and Math. with Applic.*, **46**:447–457, 2003.

- [13] J.C. Misra and S.Chakravarty. Flow of arteries in the presence of stenosis. *J. Biomech.*, **19**(11):907–918, 1986.
- [14] J.C. Misra and G.C. Shit. Blood flow through arteries in pathological state: A theoretical study. *Int. J. Eng. sci.*, **44**:662–671, 2006.
- [15] D.S. Sankar and K. Hemalatha. Pulsatile flow of Herschel-Bulkley fluid through stenosed arteries – A mathematical model. *Int. J. Non-Linear Mech.*, **41**:979–990, 2006.
- [16] M. Sharan and A.S. Popel. A two-phase model for flow of blood in narrow tubes with increased effective viscosity near the wall. *Biorheology*, **38**:415–428, 2001.
- [17] J.B. Shukla, R.S. Parihar and S.P. Gupta. Effects of peripheral layer viscosity on blood flow through the artery with mild stenosis. *Bull.Mathl.Biology*, **42**:797–805, 1980.
- [18] J.B. Shukla, R.S.Parihar and B.R.P.Rao. Effects of stenosis on non-newtonian flow of the blood in an artery. *Bull. Mathl. Biology*, **42**:283–294, 1980.
- [19] S.U. Siddiqui, N.K. Verma, S. Mishra and R.S. Gupta. Mathematical modeling of pulsatile flow of Casson’s fluid in arterial stenosis. *Appl. Math.and Comput.*, 2007. In press doi:10.1016/j.amc.2007.05.070
- [20] V.K. Sud and G.S. Sekhon. Arterial flow under periodic body acceleration. *Bull.Math. Biol.*, **47**:35–52, 1985.
- [21] C. Tu and M. Deville. Pulsatile flow of non-Newtonian fluid through arterial stenosis. *J. Biomech.*, **29**:899–908, 1996.
- [22] D.F. Young. Effects of time-depended stenosis of flow through a tube. *J. Eng. Ind. Trans. ASME*, **90**:248–254, 1968.
- [23] D.F. Young. Fluid mechanics of arterial stenosis. *J. Biomech. Eng. Trans. ASME*, **101**:157–175, 1979.
- [24] D.F. Young and F.Y. Tsai. Flow characteristic in models of arterial stenosis-II. Unsteady flow. *J. Biomech.*, **6**:465–475, 1973.